

67
Tense, JHU University Press
1985

Synchrotron Radiation: Applications to Chemistry

Albert C. Parr

Radiation Physics Division, National Bureau of Standards, Gaithersburg,
Maryland 20899, U.S.A.

Abstract

The nature and history of synchrotron radiation will be briefly covered with an emphasis on results and observations rather than a mathematical development. Several examples of the applications of synchrotron radiation as a tool to solve chemical and physical problems will be developed with sample results given. Areas of substantial research interests will be indicated along with projections on future developments.

Introduction

Synchrotron radiation was first reported by workers at the General Electric laboratory in Schenectady, NY(1,2). These workers first observed the visible portion of the radiation spectrum and noted its variance with energy of the electron synchrotron. Synchrotron radiation is an important aspect of damping and hence is related to beam stability in circular electron accelerators. The early theoretical activity in explaining synchrotron radiation was related to effects upon beam stability in these accelerators. Schwinger was the first in the U.S. to give a detailed, relativistically correct explanation of the properties of synchrotron radiation(3).

The pioneering work in the use of synchrotron radiation for use as a light source was done by Tomboulian and Hartman at the 300 MeV synchrotron at Cornell University in the early 1950's. They performed absorption spectroscopy on metals in the far UV (100-200Å) and demonstrated the usefulness of the continuous nature of the synchrotron radiation for spectroscopic purposes(4). In the early 1960's the far ultraviolet physics group at the National Bureau of Standards, led by Robert Madden, started the first systematic, sustained efforts in using synchrotron radiation for scientific studies(5). The early work on the far UV absorption in the rare gases helped launch a renewed emphasis in atomic and molecular studies as

Synchrotron Rad
well as demonstr
radiation.

During the
were establish
These include
tute for Nucle
(Physical Scie
extensively re
has devoted co
synchrotron ra

The areas
ation span al
in addition th
technological
utilize intens
ation to study
variety of spe
emitted produc
X-ray photons
and molecular
afforded by sy
unobtainable s
ture. Materia
a source of X-

1
2
3
4
5
6
7
8
9
10
11
12
13
14
15
16
17
18
19
20
21
22
23
24
25
26
27
28
29
30
31
32
33
34
35
36
37
38
39
40
41
42
43
44
45
46
47
48
49
50
51
52
53
54
55
56
57
58
59
60
61
62
63
64
65
66
67
68
69
70
71
72
73
74
75
76
77
78
79
80
81
82
83
84
85
86
87
88
89
90
91
92
93
94
95
96
97
98
99
100
101
102
103
104
105
106
107
108
109
110
111
112
113
114
115
116
117
118
119
120
121
122
123
124
125
126
127
128
129
130
131
132
133
134
135
136
137
138
139
140
141
142
143
144
145
146
147
148
149
150
151
152
153
154
155
156
157
158
159
160
161
162
163
164
165
166
167
168
169
170
171
172
173
174
175
176
177
178
179
180
181
182
183
184
185
186
187
188
189
190
191
192
193
194
195
196
197
198
199
200
201
202
203
204
205
206
207
208
209
210
211
212
213
214
215
216
217
218
219
220
221
222
223
224
225
226
227
228
229
230
231
232
233
234
235
236
237
238
239
240
241
242
243
244
245
246
247
248
249
250
251
252
253
254
255
256
257
258
259
260
261
262
263
264
265
266
267
268
269
270
271
272
273
274
275
276
277
278
279
280
281
282
283
284
285
286
287
288
289
290
291
292
293
294
295
296
297
298
299
300
301
302
303
304
305
306
307
308
309
310
311
312
313
314
315
316
317
318
319
320
321
322
323
324
325
326
327
328
329
330
331
332
333
334
335
336
337
338
339
340
341
342
343
344
345
346
347
348
349
350
351
352
353
354
355
356
357
358
359
360
361
362
363
364
365
366
367
368
369
370
371
372
373
374
375
376
377
378
379
380
381
382
383
384
385
386
387
388
389
390
391
392
393
394
395
396
397
398
399
400
401
402
403
404
405
406
407
408
409
410
411
412
413
414
415
416
417
418
419
420
421
422
423
424
425
426
427
428
429
430
431
432
433
434
435
436
437
438
439
440
441
442
443
444
445
446
447
448
449
450
451
452
453
454
455
456
457
458
459
460
461
462
463
464
465
466
467
468
469
470
471
472
473
474
475
476
477
478
479
480
481
482
483
484
485
486
487
488
489
490
491
492
493
494
495
496
497
498
499
500
501
502
503
504
505
506
507
508
509
510
511
512
513
514
515
516
517
518
519
520
521
522
523
524
525
526
527
528
529
530
531
532
533
534
535
536
537
538
539
540
541
542
543
544
545
546
547
548
549
550
551
552
553
554
555
556
557
558
559
560
561
562
563
564
565
566
567
568
569
570
571
572
573
574
575
576
577
578
579
580
581
582
583
584
585
586
587
588
589
590
591
592
593
594
595
596
597
598
599
600
601
602
603
604
605
606
607
608
609
610
611
612
613
614
615
616
617
618
619
620
621
622
623
624
625
626
627
628
629
630
631
632
633
634
635
636
637
638
639
640
641
642
643
644
645
646
647
648
649
650
651
652
653
654
655
656
657
658
659
660
661
662
663
664
665
666
667
668
669
670
671
672
673
674
675
676
677
678
679
680
681
682
683
684
685
686
687
688
689
690
691
692
693
694
695
696
697
698
699
700
701
702
703
704
705
706
707
708
709
710
711
712
713
714
715
716
717
718
719
720
721
722
723
724
725
726
727
728
729
730
731
732
733
734
735
736
737
738
739
740
741
742
743
744
745
746
747
748
749
750
751
752
753
754
755
756
757
758
759
760
761
762
763
764
765
766
767
768
769
770
771
772
773
774
775
776
777
778
779
780
781
782
783
784
785
786
787
788
789
790
791
792
793
794
795
796
797
798
799
800
801
802
803
804
805
806
807
808
809
810
811
812
813
814
815
816
817
818
819
820
821
822
823
824
825
826
827
828
829
830
831
832
833
834
835
836
837
838
839
840
841
842
843
844
845
846
847
848
849
850
851
852
853
854
855
856
857
858
859
860
861
862
863
864
865
866
867
868
869
870
871
872
873
874
875
876
877
878
879
880
881
882
883
884
885
886
887
888
889
890
891
892
893
894
895
896
897
898
899
900
901
902
903
904
905
906
907
908
909
910
911
912
913
914
915
916
917
918
919
920
921
922
923
924
925
926
927
928
929
930
931
932
933
934
935
936
937
938
939
940
941
942
943
944
945
946
947
948
949
950
951
952
953
954
955
956
957
958
959
960
961
962
963
964
965
966
967
968
969
970
971
972
973
974
975
976
977
978
979
980
981
982
983
984
985
986
987
988
989
990
991
992
993
994
995
996
997
998
999
1000

well as demonstrating the general versatility of synchrotron radiation.

During the mid 1960's, efforts in synchrotron radiation were established at a number of laboratories world-wide. These include laboratories in Italy (Frascati), Tokyo (Institute for Nuclear Studies), Hamburg (DESY Lab), and Wisconsin (Physical Science Lab). The historical developments are quite extensively reported in the literature(6-9), and Physics Today has devoted considerable space to reviews of progress in synchrotron radiation research(10).

The areas of research which now utilize synchrotron radiation span almost the entire range of scientific endeavors and in addition the synchrotron is becoming a tool in several technological areas. Solid state physics and surface physics utilize intense monochromatized light from synchrotron radiation to study order in materials as well as performing a variety of spectroscopies upon the materials and the photo-emitted products. Atomic and molecular scientists use UV and X-ray photons to probe ionization dynamics in isolated atomic and molecular systems. The intensity and wavelength range afforded by synchrotron sources have made possible heretofore unobtainable sensitive probes of atomic and molecular structure. Materials scientists have used synchrotron radiation as a source of X-rays in a variety of studies involving material

properties and in real time analysis of transformations.

Biological and medical applications include crystallographic analysis and real time analysis of reactions by monitoring shifts in x-ray absorption edges due to chemical environment. Monochromatized X-rays whose wavelength is tuned to absorption edges, can also be used for X-ray diagnostics in living systems(11,12).

The progress in the development of instrumentation for use in synchrotron radiation research is published in the conference proceedings of National and International Synchrotron Radiation Instrumentation meetings(13-16). These proceedings, plus recently published books, review in considerable detail the state of technical development and the direction of scientific research.

Table I gives a summary of U.S. synchrotron radiation facilities currently in operation. In addition to the facilities in the United States, there are approximately 25 other facilities worldwide either in operation or under construction. The size of these facilities range from small facilities such as the NBS SURF-II, which is accommodated in a large room (15mx25m) and a staff of one engineer and several technicians, to large facilities with budgets of tens of millions of dollars and a staff of several hundred people.

Synchrotron Radiation

Facility

SURF-II
 NBS, Gaithersburg,
 TANTALUS
 Wisconsin
 CESR
 Cornell, Univ.
 SPEAR
 Stanford, CA
 NSLS-VUV
 Brookhaven, NY
 NSLS-X-RAY
 Brookhaven, NY
 ALADDIN
 Wisconsin

*Adapted from R

Table 1*

Facility	E(GeV)	R(m)	I(mA)	Ec(eV)
SURF-II				
NBS, Gaithersburg, MD	.280	.83	75	59
TANTALUS				
Wisconsin	.240	.64	200	48
CESR				
Cornell, Univ.	8	32.5	100	35000
SPEAR				
Stanford, CA	4	12.7	100	11100
NSLS-VUV				
Brookhaven, NY	.7	1.9	500	400
NSLS-X-RAY				
Brookhaven, NY	2.5	8.17	500	4200
ALADDIN				
Wisconsin	1.0	2.08	500	1000

*Adapted from Ref. 19

ansformations.
 nclude crystallog-
 reactions by moni-
 e to chemical envi-
 elength is tuned to
 ay diagnostics in
 strumentation for
 ublished in the
 ernational Synchro-
 -16). These proce-
 ew in considerable
 and the direction of
 rotron radiation
 ition to the facil-
 oximately 25 other
 r under construc-
 from small facili-
 ommodated in a large
 and several techni-
 tens of millions of
 ple.

Technical aspectsSynchrotron Radiation

Synchrotron radiation can be understood from classical-relativistic electrodynamics and is, in fact, treated in standard advanced textbooks.²⁰ The concept of the origin of synchrotron radiation can be obtained by starting with the non-relativistic Larmor formula for power radiated from a charged particle in a magnetic field. The power per unit solid angle emitted by a particle of charge e is

$$\frac{dP}{d\Omega} = \frac{e^2}{4\pi c^3} |\dot{\mathbf{v}}|^2 \sin^2\theta$$

$$\text{Integrated over angle, } P = \frac{2e^2}{3c^3} |\dot{\mathbf{v}}|^2$$

where $\dot{\mathbf{v}}$, is acceleration and, θ , is angle between the acceleration (inward in our case) and the observer. The frequency of the field is the frequency of rotation. For a relativistic particle, the angular distribution becomes forward peaked along the direction of the velocity vector which is tangential to the radius of the motion. The relativistic form of the power can be written

$$P = \frac{2}{3} \frac{e^2 c}{\rho^2} \beta^4 \gamma^4$$

where ρ =radius of orbit of particle of rest mass= m and $\beta=v/c$,

$$\gamma = \frac{E}{mc^2}$$

E is the total energy of the particle.

This equation can be written

$$P = \frac{2}{3} \frac{e^2 c}{\rho^2} \beta^4 \left(\frac{E}{mc^2}\right)^4$$

Synchrotron Radiation

For equivalent energy radiated has a $1/m^4$ dependence. c are the particles of synchrotron radiation is as mentioned. If θ is direction of particle, transformed taking $\theta = 90$ in the

Even for the most massive particles $E=280\text{MeV}$

$$\gamma \approx 550$$

An observer viewing synchrotron radiation from an electron source, as a consequence, the harmonics of the Fourier components are beyond the orbital frequencies up to $\omega \sim \frac{c\gamma^3}{\rho}$ are necessary to describe the details of the spectrum. Not to be given here (18).

For equivalent energies (assumed relativistic) the power radiated has a $1/m^4$ dependence, hence electrons or positrons are the particles of choice to optimize the production of synchrotron radiation. The angular distribution of the radiation is as mentioned above, directed in the forward direction. If θ is direction of emission in the rest frame of the particle, transformation to the lab frame yields

$$\tan\theta' = \frac{\sin\theta}{\gamma(\beta + \cos\theta)}$$

taking $\theta = 90$ in the lab frame

$$\tan\theta' \cong \frac{1}{\gamma}$$

since $\beta \cong 1$

Even for the most modest storage rings such as SURF where

$E=280\text{MeV}$

$$\gamma \cong 550 \quad 1/\gamma \cong 1.8 \text{ mRad}$$

An observer viewing a tangent point will see the emission from an electron for a very brief period of time. As a consequence, the harmonic frequency range necessary to provide the Fourier components for a short pulse is greatly extended beyond the orbital frequency. Simple considerations show that frequencies up to

$$\omega \sim \frac{c\gamma^3}{\rho} \quad \text{or for an energy, } \epsilon = \hbar\omega = \frac{\hbar c\gamma^3}{\rho}$$

are necessary to provide the short pulse observed.¹⁸ The details of the spectral distribution are involved and will not be given here but can readily be found in the literature(18).

The critical energy, $\epsilon_c = 3hc\gamma^3/2\rho$, is an energy near the maximum in spectral intensity. For high energy machines such as CESR at Cornell, $E=8\text{GeV}$ and $\epsilon_c=35\text{keV}$, which is in the X-ray range. For SURF $E=.24\text{GeV}$ and $\epsilon_c=37\text{eV}$, an energy in the far ultraviolet. Figure 1 gives the spectral brightness per millimeter of beam height for the several storage rings in the United States. For more details refer to the original literature (17-20).

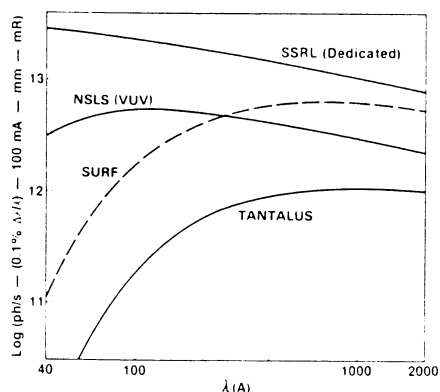
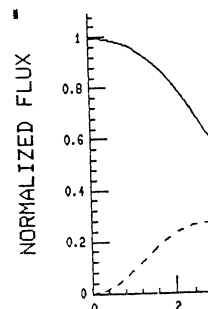


Fig. 1 Flux of US VUV storage rings in photons/sec .1% bandpass-100mA-mm (beam height). The beam height used was SSRL=.2mm, NSLS=.4mm, SURF=.1mm, Tantalus=.5mm.

In the plane of the orbit, the synchrotron radiation is linearly polarized. Above and below the plane of the orbit, the polarization is elliptical and has a wavelength and energy dependence. The normalized flux of the parallel and perpendicular components of the intensity from SURF at 1500Å is shown in Fig. 2. For shorter wavelengths the distribution

Synchrotron Radi
narrows with a c
perpendicular co



As a pract
tron radiation
is stored in a
focusing devic
ular and beam
net. Given a
stored electro
The stora
iary electron
further accele
bending magne
electrons wit

MEMB
Indis
CCP
MUSTO

narrows with a corresponding decrease in the amount of perpendicular component.

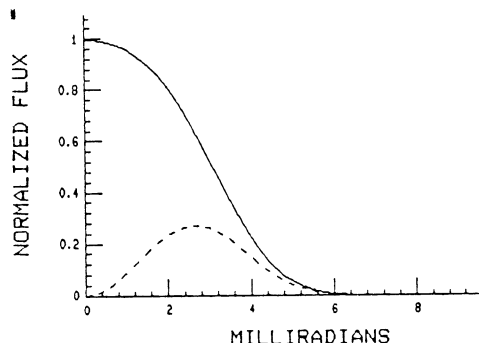


Fig. 2 The normalized flux of the perpendicular and parallel components of the intensity of 1500Å light from SURF. In the plane of the orbit the light is 100% parallel polarization.

As a practical strategy for the generation of synchrotron radiation, a beam of high energy electrons or positrons is stored in a "ring" and focused by bending magnets and focusing devices. SURF is unique in that the orbit is circular and beam confinement accomplished by a single large magnet. Given a sufficiently good vacuum, the lifetimes of stored electron beams can be many hours.

The storage ring itself is usually injected by an auxiliary electron accelerator. The captured beam can then be further accelerated by increasing the magnetic field of the bending magnets and relying upon the phase stability of the electrons with the applied R.F. field to increase the energy

of the beam and to maintain focus(21). The phase stability of the beam also leads to the bunching of the electrons along the orbit. For a large machine the frequency of the R.F. cavity may be many times the orbital frequency which results in many bunches being in the storage ring simultaneously.

Beamlines

Synchrotron radiation from a tangent point of the beam in the magnet is directed onto optical components which can disperse and deflect the beam. The vacuum and safety requirements to maintain storage ring integrity give rise to stringent requirements on the development of the beam transport system. The large flux of X-rays and VUV (vacuum ultraviolet) photons on the entrance optics creates technical difficulties. For example, oil from mechanical pumps can reach the optics of an instrument. The X-rays and VUV photon then can photodissociate the hydrocarbons leaving as a residue, a carbon (graphite) type deposit.²² This contamination can severely degrade the performance of the optical elements, necessitating expensive replacement or time-consuming cleaning procedures. In high energy rings such as NSLS X-ray, CHESS or SSRL, the radiation load itself can constitute a significant technical problem. For example at the NSLS X-ray ring, the total power radiated per horizontal milliradian for an operating current of 250mA is about 17 watts/milliradian. Hence an optical

Synchrotron Radiation device can easily i power scales direct operating currents quence, materials s ing of the initial factors have create with a resultant re

The schematic which is installed

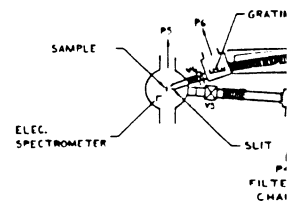


Fig. 3 Diagram of S1-S4 are radiation shutters to isolate P1-P6 are ultrahigh a series of valves itself. The front-vacuum interfacing bers. This section

device can easily intercept a hundred or more watts. The power scales directly with the beam current and hence larger operating currents increase the radiation load. As a consequence, materials such as silicon carbide(23) or external cooling of the initial optical element may be required. These factors have created new challenges to the optical designer with a resultant renaissance in optical engineering. The schematic drawing in Fig. 3 shows a typical beamline which is installed at NSLS(24). The experiment is isolated by

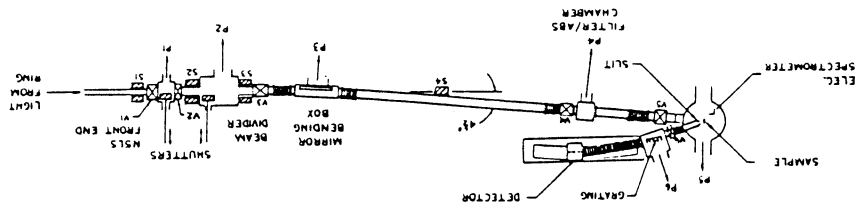


Fig. 3 Diagram of ORNL-UT-NBS soft x-ray beamline at NSLS.

SI-S4 are radiation shields; VI-V6 are vacuum valves and shutters to isolate the experimental region from the ring. PI-P6 are ultrahigh vacuum pumps.

a series of valves and chambers from the storage ring source itself. The front-end (nearest the storage ring) provides vacuum interfacing and accident containment valves and chambers. This section has been engineered by the storage ring

staff according to their vacuum and contamination requirements. The front-end may also provide a dividing arrangement to portion parts of the accepted radiation to several different beamlines. The beamline in Figure 3 features horizontal and vertical focusing, grazing incidence mirrors. This particular beamline uses the undispersed synchrotron radiation to impinge upon a sample and then uses a 5 meter grazing incidence spectrograph to view the x-ray fluorescence. Different types of experiments might require a dispersed light source for the experiment in which case a monochromator would come before the sample region.

Ultra-high vacuum requirements are now the general rule at most storage ring facilities. This requires a minimum of flexible elastometer seals and the reliance upon ion pumps, closed cycle helium cryopumps, and in some instance carefully baffled and maintained turbomolecular pumps. Experiments which require a high pressure in the sample region must then be isolated from the monochromators and transport lines by a suitable vacuum window or by adequate differential pumping.

A typical storage ring will have many beamlines constructed for various experiments in a variety of wavelength regions spanning the spectral range from the infrared to the X-ray. Quite often the storage ring facility provides the use of monochromators and beamlines so that a prospective user

Synchrotron R.

only needs to

Monochromator

Monochro

for use at s

challenges h

size, and hi

To take adva

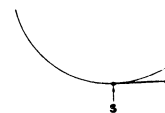
synchrotron

chromators h

toroidal foc

focusing ove

well has unc



LEGEND: C
CP
DS
E
ES
B

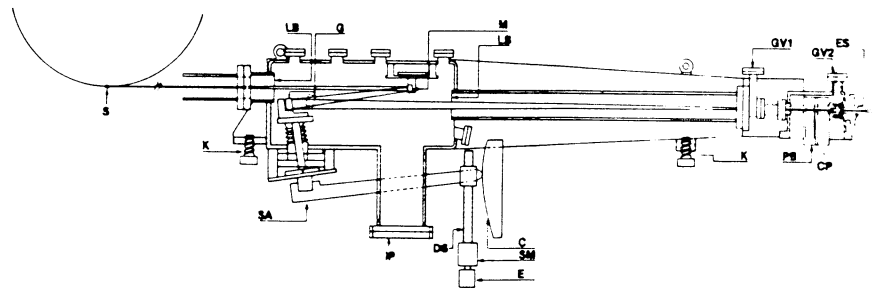
Fig. 4 2

only needs to provide the actual experimental apparatus.

Monochromators and Optics

Monochromator design has undergone significant changes for use at synchrotron radiation sources(13-15). The basic challenges have been to adapt to the high fluxes, small source size, and high vacuum requirements offered by storage rings. To take advantage of the shorter wavelengths available with synchrotron radiation, new types of grazing incidence monochromators have been designed, some of which take advantage of toroidal focusing elements to achieve better approximate focusing over extended wavelength regions. X-ray optics as well has undergone a major change and improvement due to the

HIGH THROUGHPUT NORMAL INCIDENCE MONOCHROMATOR AT SURF-II



LEGEND:	C	CAM	GV1	GATE VALVE	S	SOURCE
	CP	CRYOPUMP	GV2	WINDOWED VALVE	SA	SCANNING ARM
	DS	DRIVE SCREW	IP	ION PUMP	SM	STEPPING MOTOR
	E	WAVELENGTH ENCODER	K	KINEMATIC MOUNT		
	ES	EXIT SLIT	LB	LIGHT BAFFLES		
	G	GRATING	PB	PUMP BAFFLES		

Fig. 4 2 meter normal incidence monochromator at SURF

opportunities and demands of synchrotron sources(25).

An example of a monochromator designed particularly for synchrotron radiation is shown in Fig. 4. This monochromator was designed by scientists at NBS for use in the wavelength region of 350A to 2000A. (26) The optics images the synchrotron beam (s) directly, without benefit of entrance slits. This allows for maximum flux throughput and to a degree simplifies the optics. A plane mirror (M) reflects the incident light from the storage ring back onto the grating (G). The light is then dispersed and focused on the exit slit (ES). The monochromator vacuum vessel is separated from the experiment by a differential pumping chamber which is pumped with a cryopump. Depending upon the experiment, the light can be used directly or transported for up to several feet with a light pipe consisting of a capillary tube.

Experiments have been performed, using the vacuum isolation given by the capillary, in which the pressure in the experimental chamber was 10^{-4} torr, and yet maintaining a pressure of several times 10^{-9} torr in the monochromator. The monochromator is pumped with an ion-pump as is the storage ring itself. The care in vacuum technology and cleanliness results in a virtually hydrocarbon-free monochromator with long optical component lifetimes. This monochromator has standard metal seal flanges at the exit region and hence will

Synchrotron

accept a v
the user,
to 2000Å.
throughput
be expected
this monochromator
worldwide.

To obtain
shorter than
incident radiation
focusing efficiency
normal incidence
such as to
matism. O
mirrors have
has its at
source chamber
available

Scientific

Two a
viewed in
brief description
synchrotron

Albert C. Parr

Synchrotron Radiation: Applications in Chemistry

175

sources(25).

particularly for
his monochromator
in the wavelength
ranges the synchrotron

ice slits. This
degree simplifies

incident light
(G). The light is

t (ES). The mono-
he experiment by a

d with a cryopump.
n be used directly

a light pipe

the vacuum isola-
pressure in the

maintaining a
monochromator. The

is the storage
and cleanliness

monochromator with
chromator has

region and hence will

accept a variety of experiments and can, from the viewpoint of the user, be considered as a continuous light source from 350Å to 2000Å. Grating changes and choice affects the overall throughput, but fluxes on the order of 10^{10} photons/sec-Å can be expected under normal operating conditions. Variants of this monochromator are at use in other synchrotron facilities worldwide.

To obtain significant fluxes of radiation at wavelengths shorter than 400Å, it becomes advantageous to utilize grazing incident reflections from the optical components. Spherical focusing elements, due to their severe astigmatism for non-normal incidence, are replaced by more complicated surfaces such as toroids which, to a degree, correct some of the astigmatism. Other optical designs with plane grating and focusing mirrors have been explored and instruments built. Each design has its attributes for particular experimental problems and source characteristics as well as financial and, perhaps, available space issues(27).

Scientific Applications of Synchrotron Radiation

Two applications of synchrotron radiation will be reviewed in some detail and some other applications in a more brief descriptive manner. Since the wavelength region of synchrotron radiation is large, i.e. from the infrared to the

X-ray, the class of experimental activities is correspondingly large and cannot be reviewed in substantial detail here.

Applications to molecular photoionization dynamics with regard to studying shape resonances and autoionization and research in surface science, using photon stimulated desorption and photoemission, will be summarized along with references to other applications.

Molecular photoionization

Experimental techniques

The photoionization program uses the 2 meter normal

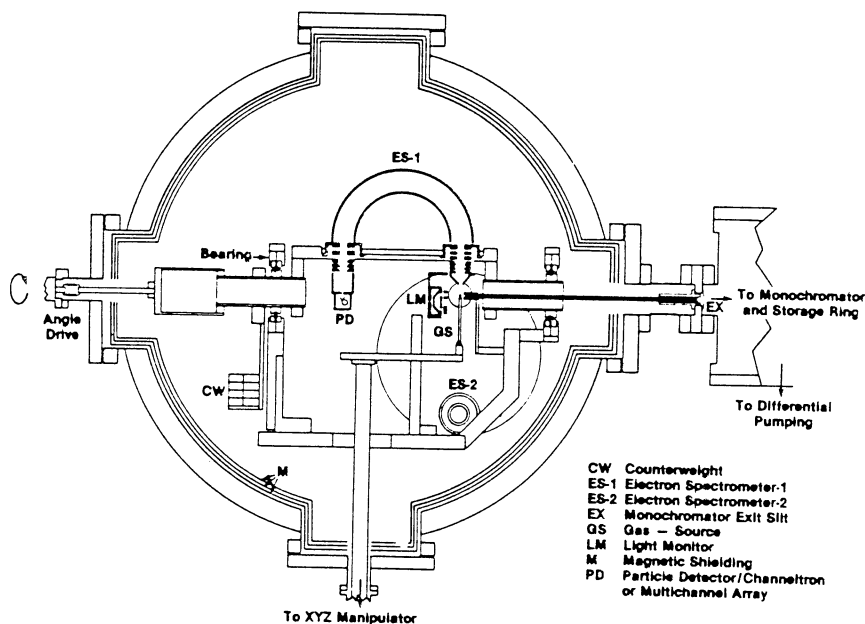


Fig. 5 High resolution ARPES experiment at SURF II. Basically the instrument consists of two 10 cm mean radius hemispherical electron energy analyzers.

Synchrotron Rad
 incidence mono
 electron spect
 angular distrib
 rent version of
 Fig. 5. The re
 50 meV under no
 achieved for hi
 monochromator c
 electric dipole
 a process can b

where

σ_V = Total cross

β_V = Asymmetry p

P = Polarizatio

Θ = Angle betwe

emit-ted el

Figure 6 shows th

process. The num

constant solid ar

the differential

equation can be r

$N(\Theta)$

incidence monochromator (Figure 4) at SURF coupled to a photoelectron spectrometer which is capable of monitoring the angular distributions of the emitted photoelectrons. The current version of the photoelectron spectrometer is shown in Fig. 5. The resolution of the electron spectrometers is about 50 meV under normal operating conditions but 20 meV can be achieved for high resolution experiments. The bandpass of the monochromator can be varied, but is typically .5Å. For an electric dipole transition the differential cross section for a process can be written

$$\frac{d\sigma_v}{d\Omega} = \frac{\sigma_v}{4\pi} \left[1 + \frac{\beta_v}{4} [3P\cos^2\Theta + 1] \right]$$

where

σ_v = Total cross section for a particular vibronic transitions

β_v = Asymmetry parameter for a particular vibronic transition

P = Polarization of light

Θ = Angle between electric field vector of the light and emitted electron.

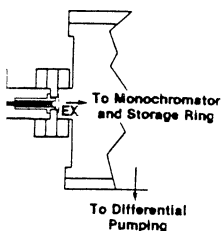
Figure 6 shows the kinetic parameters of the photoionization process. The number of electrons measured by a detector of a constant solid angle of acceptance, $N(\Theta)$, is proportional to the differential cross section, hence the cross section equation can be recast.

$$N(\Theta) = N_{0v} \left[1 + \beta_v / 4 [3P\cos^2\Theta + 1] \right]$$

s correspondingly
etail here.

amics with regard
on and research
esorption and
references to

ter normal



nterweight
:ron Spectrometer-1
:ron Spectrometer-2
ochromator Exit Silt
- Source
t Monitor
netic Shielding
icle Detector/Channeltron
ultichannel Array

RF II. Bas-

an radius hemi-

appropriate molecular models and hence the parameters can be used as a direct test of theory. The necessity of theory to correctly calculate matrix elements (cross section) and relative phases of matrix elements (asymmetry parameters) is a more stringent condition than cross section alone. The vibrationally resolved data additionally tests the accuracy of the approximations involved in calculating electronic properties at a fixed intermolecular configuration and the assumptions regarding the separation of the various motions of a molecule(29).

Gas samples are introduced into the interaction region with an effusive aperture. The pressure differential between the experimental chamber and the monochromator, maintained by a glass capillary, is on the order of 10^4 . The chamber has 3 layers of internal magnetic shielding with a resultant internal field of on the order of one milligauss. The system is pumped by a turbopump and closed cycle helium refrigerator cryopumps(30).

Shape Resonance in Nitrogen

Shape resonances derive their name from the fact that they result from the shape of the molecular potential. In the cases studied so far the shape resonance results from a centrifugal barrier, which for certain ranges of kinetic

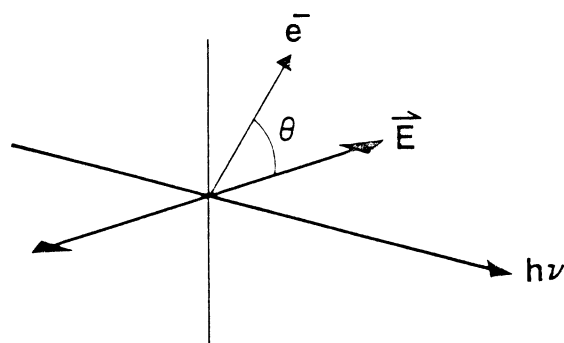


Fig. 6 Schematic of photoemission process.

The polarization, P , is measured in a separate experiment by a three mirror polarization analyzer(28), and hence a measurement of $N(\theta)$ at two separate angles determines No_v and β_v . No_v can be normalized to the total number of electrons in a given band and hence can be directly related to the partial cross section for a given vibronic process. The asymmetry parameter β_v is a measure of the departure from isotropy of the outgoing electron angular distribution. The β parameter is related to the angular momentum composition of the electron wavefunction. In a situation in which there is more than one possible ionization channel (for example $np \rightarrow \epsilon d, \epsilon s$) the asymmetry parameter is related to the relative phases of the outgoing channels. No_v and β_v can be calculated by using

Synchrotron Radi

appropriate mole
used as a direct
correctly calcul
tive phases of π
more stringent c
tionally resolve
approximations i
at a fixed inter
regarding the se
molecule(29).

Gas samples
with an effusive
the experimental
a glass capillar
layers of intern
nal field of on
pumped by a turbo
cryopumps(30).

Shape Resonance i

Shape resonanc
they result from
the cases studied
centrifugal barri

energy can affect the motion of the photoemitted electron. The centrifugal barrier is dependent upon the angular momentum composition of the final state of the exiting electron and hence in general the effect would not appear in every ionization channel. In molecular nitrogen, for example, there is a shape resonance in the $3\sigma_g + \epsilon\sigma_u$ channel but not in the other ionization channels. This process leaves the N_2^+ molecule in its ground ionic state ($X^1\Sigma^+_g$). The same shape resonance appears in the k-shell x-ray absorption spectra and manifests itself with a rapid rise in the σ_u partial cross section at a kinetic energy of about 1 Rydberg (13.6eV)(29). Calculations show that the continuum f-wave penetrates into the region of the molecular core at a kinetic energy of about 1 Rydberg with a rapid increase in amplitude and a corresponding phase shift of π (31).

The result is that at about 1 Rydberg kinetic energy in the σ_u channel the outgoing electron is temporarily trapped. This trapping produces a drastic departure from Franck-Condon predictions in the vibrational intensities(32). In part this disruption of Frank-Condon predictions is due to the rapid variation in the detailed form of the molecular potential as a function of internuclear distance. Shape resonances can then affect different vibrational transitions in different ways. Experimentally, then, the effects of shape resonance phenomena

Synchrotron Radiation:

can be tested by measure
ous vibrational transiti
asymmetry parameters are
presence of resonance ph
relative phases of the c
is dependent upon molecu

The experimental re
for the branching ratio
gen ion ground state is
experimental data taken
multiple scattering mode
a frozen core Hartree-Fc
tion(35), and the double

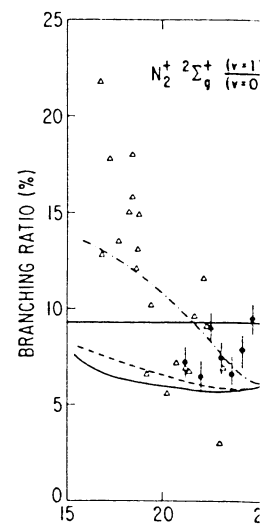


Fig. 7 Branching ratio c
region of shape resonance

can be tested by measurements of the branching ratios to various vibrational transitions. The measurement of the angular asymmetry parameters are also useful in demonstrating the presence of resonance phenomena as they are sensitive to the relative phases of the outgoing partial wave composition which is dependent upon molecular configuration and potential.

The experimental results and the results of calculations for the branching ratio of the $V=1$ to $V=0$ levels of the nitrogen ion ground state is shown in Fig. 7. The solid data are experimental data taken at NBS(33), the dot-dash the result of multiple scattering model prediction(34), the solid line from a frozen core Hartree-Fock level dipole-length calculation(35), and the double-dash line the Hartree-Fock frozen

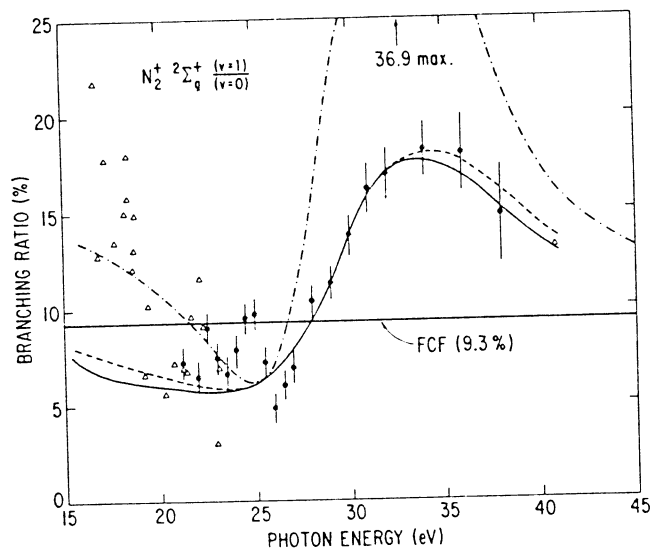


Fig. 7 Branching ratio of N_2 $V=1$ to $V=0$ photoionization in region of shape resonance. See text for explanation.

core dipole-velocity approximation. The triangles are experimental points from Gardner and Samson(36). The multiple scattering model calculation was the first to predict the observed effect but over-estimated the magnitude. The Hartree-Fock calculation using a more realistic potential, within a self-consistent framework, gives a more accurate description of the phenomena. The lack of agreement between the calculations and the data at energies below 25 eV is most certainly due to autoionizing phenomena which are not accounted for in either picture. The asymmetry parameter for the predicted vibrational state dependence was measured by Carlson and his co-worker at the University of Wisconsin storage ring and is in substantial agreement with the theoretical predictions(37). Recent work at NBS at improved resolution and data density confirms the conclusion of Carlson and his co-workers.

The shape resonance phenomenon is not an isolated occurrence and in fact has been seen in a wide range of molecular systems which include diatomic molecules such as CO, N₂, and NO and larger species including SF₆, BF₃, C₂H₂, and CO₂(29). This application of synchrotron radiation to study shape resonance phenomena has taken place at a number of laboratories throughout the world. The result has been an improved theoretical understanding of the photoionization process as well as adding significantly to the body of experimental fact.

Autoionization

Autoionization of a neutral system. For example, ionization occurs in which two electrons are excited and the energy of one exceeds the ionization energy of the excited state. The excited state is above the ionization continuum. As a result, there can occur a characteristic autoionization process. The motions of the electrons cannot be regarded as independent. This, which is an unwelcome phenomenon, provides insights into molecular systems. The phenomenon was subject worth studying. Photoionization phenomena.

Autoionization in Molecular Nitrogen

Autoionization occurs when a discrete electronic state of a neutral system lies above the ionization limit of the molecule. For example in a simple system such as Helium, autoionization occurs from transitions such as $\text{He}(1s^2) \rightarrow \text{He}(2s2p)$ in which two electrons are simultaneously excited and their energy exceeds the first ionization potential of the molecule. The excited state interacts with the continuum with the result that the quasi-bound state decays into the ionization continuum. As a consequence, in the continuous absorption region above ionization onset in atomic and molecular systems, there can occur discrete-like absorption minima or maxima with a characteristic resonance-like profile(38). The autoionization process results from the correlation of the motions of the various electrons in an atom or molecule and cannot be readily understood within a single electron picture. This, which in some circumstances could be considered an unwelcome problem, can be also viewed as a window to gain insights into the nature of correlation in atomic and molecular systems. Correlation between electrons is the central phenomenon which gives rise to chemical bonding and hence is a subject worthy of study.

Photoelectron spectroscopy can be used to study autoionization phenomena by studying the branching ratios to various

state. Most molecular systems exhibit considerable autoionization in the first 10-20eV above ionization onset. Molecular nitrogen is a particularly good example in that there are several well resolved series of prominence of which the Hopfield emission and absorption series are a good example(39,40). Figure 8 shows the vibrational branching ratios for the first four levels of the ground ionic state and Fig. 9 the asymmetry parameters for the four levels. The wavelength region shown covers the range of the first member (principal quantum number = 4) for the Hopfield series. There is a window resonance (absorption minima) at about 715Å and an absorption maxima at about 723Å (vertical line in figure). The thing to note is the rapid and large variations in the branching ratios and the asymmetry parameters. The $V=0$ vibrational level loses amplitude relative to the weaker peaks and departs significantly from constant Frank-Condon predictions. The lifetime and configuration of the intermediate state, the autoionizing level, is reflected in this changed distribution. A treatment based upon multichannel quantum defect theory (MQDT) by Raoult and co-workers gives substantial agreement with the experiment(41). Keeping in mind that the maximum range of values for the asymmetry parameter is -1 to +2, the variations observed in Fig. 9 are significant and represents rapid, drastic variation in the

vibrational transitions and the corresponding asymmetry parameters. Since autoionization results from a coupling of the continuum (or several continua) and a discrete-like state, the cross sections and the phase of the outgoing electron wavefunction can undergo local variations in the neighborhood of the resonance. This region of the resonance can be from a very narrow region ($\Delta E < 1 \text{ meV}$) to one as large as many electron volts, depending on the lifetime of the discrete-like

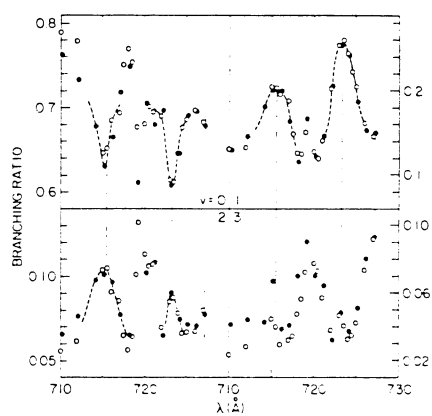


Fig. 8 The branching ratios of the first four vibrational levels in $N_2^+ x$ state in the region of the $m=4$ Hopfield Series.

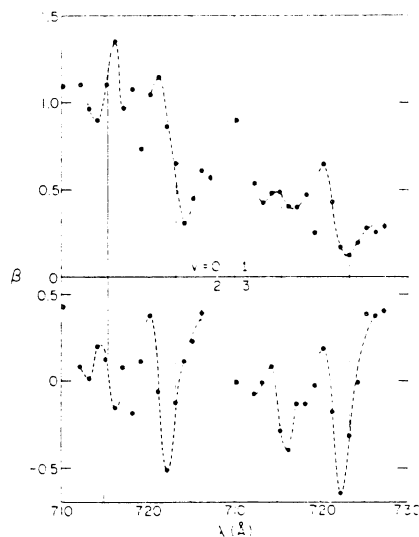


Fig. 9 The asymmetry parameters for the first four vibrational levels of the $N_2^+ x$ state in the region of the $m=4$ Hopfield Series.

Synchrotron Radiation state. Most molecular ionization in the first nitrogen is a part of several well resolved Hopfield emission lines (39,40). Figure 8 for the first four vibrational levels shows the asymmetry parameter in this region shown covering the quantum number = 4. The observed resonance (absorption maxima at about 710-720 Angstroms) is something to note is that the branching ratios at the vibrational level and departs significantly from the predictions. The intermediate state of this changed distribution of multichannel quantum states gives substantial evidence. Keeping in mind that the asymmetry parameter is a measure of the relative contributions of the various channels, these are significant and

angular distributions of electrons in the regions of autoionizing resonances.

The body of information on the effects of autoionization in photoionization is growing rapidly, primarily due to the availability of synchrotron sources worldwide. These studies along with the study of ionization phenomena due to inner shell excitation, will be an important area of research to investigate the nature of electron dynamics in atomic and molecular systems.

Surface Science and Solid State Physics

There has been a tremendous impact upon research in surface science and solid state physics by synchrotron radiation. The intense monochromatic light from storage rings can be used to perform multiple spectroscopies with heretofore unobtainable sensitivity. For example the detailed study of the absorption of X-rays in solid samples and the observation of fine structure in the absorption has led to the development of what is now called extended X-ray absorption fine structure (EXAFS). The EXAFS structure results from the periodicity of the sample and the scattering of outgoing waves by multiple spatially correlated scattering centers(42). This research has developed into a major enterprise in its own right, with efforts at almost every storage ring.

Synchrotron Radiation:

Figure 10 demonstrates the use of synchrotron radiation on a storage ring. The sample, mounted on a crystal, is mounted and biased. Photons are incident upon the sample. The detector, with the cylindrical

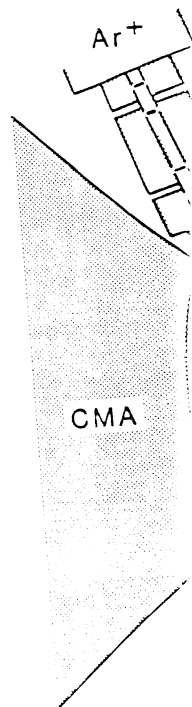


Fig. 10 Schematic of synchrotron radiation use on a storage ring.

Figure 10 demonstrates a typical configuration for studying surfaces of samples. The sample, usually a single crystal, is mounted on a manipulator with leads for heating and biasing. Photons enter from a monochromator (P) and fall upon the sample. The photoemission spectra can be measured with the cylindrical mirror energy analyzer (CMA), which is

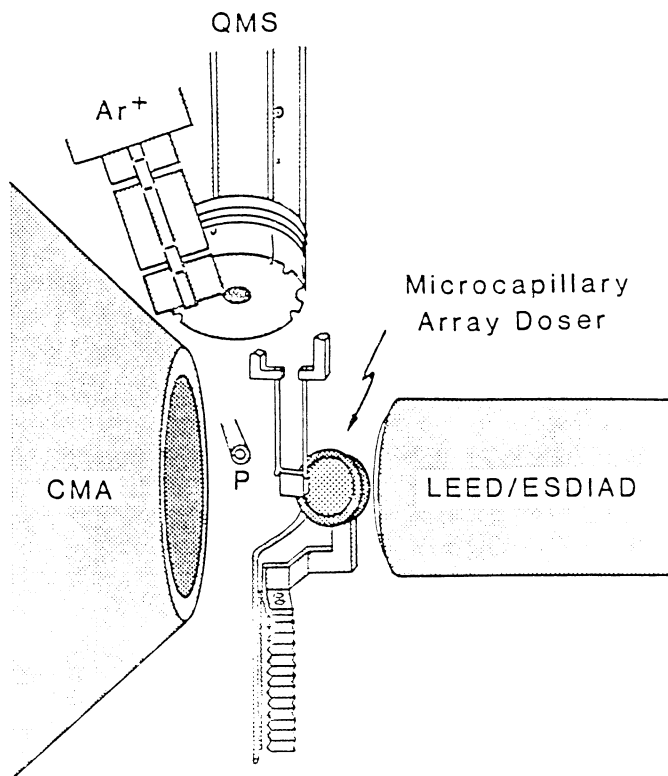


Fig. 10 Schematic of a typical surface science apparatus for use on a storage ring. See text for explanation of symbols.

also used to analyze the ions from photon stimulated desorption (PSD). An Argon ion gun (AR) is used for cleaning the surface. The quadrupole mass spectrometer (QMS) is used for analyzing the residual gas in the vacuum chamber or for checking the purity of the sample gas to be adsorbed on the surface. Low energy electron diffraction (LEED) is used for monitoring surface order as well as an indicator of coverage of the surface by sample gases. The LEED device can also be used to view the electron stimulated ion angular distribution of (ESDIAD), which can be used in conjunction with the PSD studies to obtain information on the nature of the surface molecular bonding. To view directly the angular distribution of the ions from PSD, a separate apparatus must be used because of, in part, signal to noise problems. A device called an ellipsoidal mirror analyzer is being constructed for use in such studies and is described in the literature(43,44).

The mechanisms of desorption of species from surfaces involve indirect pathways since the momentum of the photon or electron is insufficient to dislodge adsorbed species directly. These mechanisms, which can be different for ions and neutrals, have been reviewed recently in the literature(45). The cross sections for reactions leading to desorption are small, several orders of magnitude below that of equivalent gas phases reactions. A modified Frank-Condon type argument,

the Menzel-Gor
the primary o
The desorptio
Feibelman mod
tron by the
decay by aug
process can
species and
ing site.
two, with t
face region
Since the f
cite are a
will exit
the bond a
cies can
patterns,
be studie
deduce a
well as r
binding.
Fig
the tung
pattern

the Menzel-Gomer-Redhead (MGR) model(46) accounts for many of the primary observations of the desorption of neutral species. The desorption of ionic species is described by the Knotek-Feibelman model which considers the excitation of a core electron by the incoming photon or electron and the subsequent decay by auger processes of the bonding electrons (47). The process can result in several positive charges on the adsorbed species and a corresponding positive charge on a nearby bonding site. This results in a coulomb repulsion between the two, with the result, that adsorbed species can exit the surface region with several electron volts of kinetic energy. Since the forces between the adsorbed species at the bonding site are along the internuclear axis, the adsorbed species will exit the surface region in a direction corresponding to the bond angles. Viewing of the pattern of the desorbed species can give a map of bonding nature of the system. These patterns, as well as change in the photoemission spectra, can be studied as a function of coverage and photon energy to deduce a picture of the surface-adsorbate configuration as well as notions about the nature and composition of the binding.

Figure 11 shows a PSD pattern of O^+ ions desorbed from the tungsten (111) plane at a photon energy of 44.3 eV. The pattern reflects a threefold symmetry of the oxygen bonded to

New Dirn
Edited by I
As the "ce
for the qu
substances
ments in it
the paper
symposium
Industry-U
at Texas A
Tilica
are the toll

New Dirn
The Role o
Molecular
Road

Investigate
Zoolites by
Colin

Recent Ad
Robot

The Migr
Chromatog
Preparative
Coory

Fourier Tr
Alan

Electrode
A. T.

Synchrotr
Albert

Flow layer
Concept of
Laser

NUMBER 11
the Index
(ILCCP) o
Chemistry.



(b) $h\nu = 44.3 \text{ eV}$

Fig. 11 Ion angular
distribution from photon
stimulated desorption of
 O^+ from tungsten oxide.

the tungsten substrate(48). These patterns are produced by the ellipsoidal mirror analyzer mentioned above (43) which images the desorbed ions on an image intensifier system. Images can be made as a function of photon energy and coverage. The ion intensities vs photon energy roughly follow the secondary electron yield, which would be indicated by the Knoteck-Feibelman model as the secondary electron yield reflects the rate of core hole formation. An example of this is shown by a PSD study of the Ti(001) surface by Stockbauer et al.(49). The ion yields of H^+ from a Ti(001) surface covered with OH is shown in Fig. 12. Also shown are the secondary electron yield and results for O^+ desorbed from an oxygen

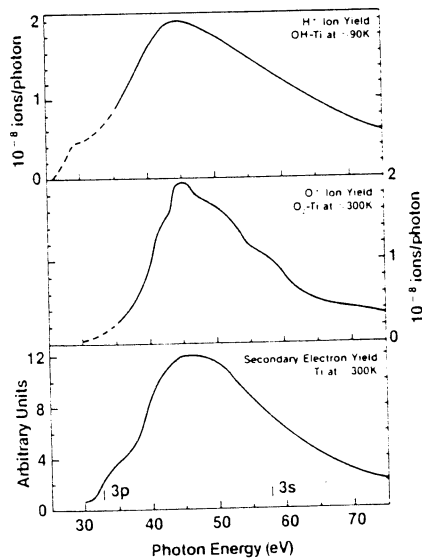


Fig. 12 Secondary electron yield and ion yields from Ti, titanium oxide, and water covered titanium.

covered surface. The high energy portions of all the yields are the same but differ substantially on the low energy side. In particular the O^+ desorption has an onset in the 3p core hole region whilst the H^+ from the OH covered Ti has an onset 5 eV or so lower. It is thought that this suggests that some of the H^+ desorption comes from (OH) bonding sites and that the lower onset corresponds to core hole (2s) formation in oxygen.

This brief space only allows for a sampler of the diverse projects and scientific accomplishments achieved in solid state physics and surface science with the advent of synchrotron radiation sources.

Albert C. Parr

angular
from photon
absorption of
titanium oxide.

produced by
(43) which
system.
and cover-
follow the
by the
yield re-
e of this is
Schockbauer et
surface covered
secondary
oxygen

Source (ALS), has been suggested for material research and other application at the Lawrence Berkeley Laboratory.

Acknowledgements:

The author wishes to thank the operation crew at the NBS storage ring for their help over the years to achieve some of the scientific results reported here. Also considerable thanks is tendered to my colleagues, Drs. Stockbauer, Madey, Ederer, Southworth, and Dehmer for the assistance and support over the years. The Office of Naval Research has supported in part the work described here.

References

1. Blewett, J.P.; Phys. Rev. (1946), 69, 87.
2. Elder, F.R.; Gurewitsch, A.M.; Langmuir, R.V.; Pollock, H.C. Phys. Rev. (1947) 71, 829.
3. Schwinger, J. Phys. Rev. (1946) 70, 798.
ibid Phys. Rev. (1949) 75, 1912
4. Tomboulion, D.H. and Hartman, P.L. Phys. Rev. (1954), 95, 600. Phys. Rev. (1956) 102, 1423.
5. Madden, R.P. and Codling K. Phys. Rev. Lett. (1963) 10, 516. This was the first in a series of publications from NBS involving the use of synchrotron radiation.
6. Lea, K.R. Phys. Reports (1978) 337 43,

7. Winich H. of S. Doniach "Overview of Synchrotron Radiation Research" in Synchrotron Radiation Research, ed. by Winick and Doniach, Plenum Press, New York, 1980.
8. Rowe, E.M. Physics Today 1981 28, 34 (May issue).
9. See articles in "Synchrotron Radiation" ed. by Eastman D.E. and Farge, Y. North Holland Pub. Company, Amsterdam, 1983.
10. See the following issue of Physics Today: May 1981, June 1983, March 1984, April 1984, for discussions of historical, technical, and scientific issues, which are written for the non-specialist.
11. Zeman, H.D.; Hughes, E.B; Campbell, L.; Hofstader, R.; Hudson, A.; Otis, J.N; Rolfe, J.; Rubenstein, E.; Harrison, D.C.; Kenoff, R.S.; Thompson, A.C.; Brown, G.S. Nucl. Inst. and Meth. (1984), 308, 222.
12. Thompson, A.C.; Llacer, J.; Campbell-Finmas, L.; Hughes, E.B.; Otis, J.N.; and Zeman, H.D. Nucl. Inst. and Meth. (1984), 319, 222.
13. "Synchrotron Radiation Instrumentation. Ed. by Ederer, D.L. and West, J.B. published as Nucl. Instr. and Meth. (1980) 122 by North Holland Publishing Corp., Amsterdam.

14. "Synchrotron Conference" E
lished in Nucl
Holland Pub.
15. "Synchrotron
ference" Ed.
lished in Nucl
Holland Pub.
16. Proceedings
VUV Synchro
Nucl. Inst.
published by
17. "Synchrotron
edited by C.
18. "Synchrotron
Doniach, S.,
19. "Handbook on
North Hollan
20. Jackson, J.D
Wiley and So
18
21. Livingood, J
ators", Van

Albert C. Parr

Synchrotron Radiation: Applications in Chemistry

195

14. "Synchrotron Radiation Instrumentation 2nd National Conference" Ed. by Mills, D.M. and Batterman, B.W., Published in Nucl. Inst. and Meth. (1982), 195, by North Holland Pub. Corp., Amsterdam.
15. "Synchrotron Radiation Instrumentation 3rd National Conference" Ed. by Thomlinson, W. and Williams, G.P., published in Nucl. Inst. and Meth. (1984), 222 by North Holland Pub. Co., Amsterdam.
16. Proceedings of the International Conference on X-ray and VUV Synchrotron Radiation Instrumentation", published in Nucl. Inst. and Meth. (1983) 208 ed. by Koch, E.E. published by North Holland Pub. Co, Amsterdam.
17. "Synchrotron Radiation: Technique and Applications" edited by C. Kunz, Springer-Verlag, Berlin (1979).
18. "Synchrotron Radiation Research" ed. by Winnick, H. and Doniach, S., Plenum Press, New York, 1980.
19. "Handbook on Synchrotron Radiation" ed. by E.E. Koch, North Holland Pub. Co., Amsterdam 1983.
20. Jackson, J.D. "Classical Electrodynamics" 2nd ed. John Wiley and Sons Inc. New York, 1975. See also ref. 3, 17, 18
21. Livingood, J.J. "Principles of Cyclic Particle Accelerators", Van Nostrand, Princeton, NJ 1961.

22. Boller, K.; Haelbich, R.P.; Hogrefe, H.; Jark, W.; and Kunz, C. Nucl. Inst. Meth. (1983), 208, 273.
23. Kelly, M.M. and West, J.B. Proc. SPIE, Inst. Soc. Opt Eng. (1981), 315
24. Callcott, T.A., Ederer, D.L., Arakawa, E.T., SPIE, (1984), 61, 447.
25. See for example the review by Underwood, J. and D. Atwood, Physics Today, April 1984 p. 44.
26. Ederer, D.L., Cole, B.E., and West, J.B., Nucl. Inst. and Meth. (1980), 172, 185.
27. See chapter by Gudat, W. and Kunz, C. titled "Instrumentation for Spectroscopy and Other Applications" in Ref. 17.
28. Horton, V.G.; Arakawa, E.T.; Hamm, R.N.; Williams, M.W. Appl. Opt. (1969), 8 617.
29. Dehmer, J.L.; Dill, D.; Parr, A.C. "Photoabsorption of Small Molecules" in Photophysics and Photochemistry in the Vacuum Ultraviolet, ed by McGlynn, S.; Findley, G.; Heubner R. D.; Reidal Pub. Comp., Dordrecht, Holland, 1984
This article reviews the current theoretical and experimental progress in photoionization processes.
30. Parr, A.C.; Southworth, S.H.; Dehmer, J.L.; Holland, D. Nucl. Inst. Meth. (1984), 222, 221.

31. Dehmer, J. 213. See problem.
32. Herzberg, Nostrand (contains an molecules transition
33. West, J.B. Stockbauer L105.
34. Dehmer, J. (1979) 43
35. Lucchese, 2166.
36. Gardner, (1978), 1
37. Carlson, Grimm, F.
38. Robert D. Spectra." 1981. Th extensive offers an to the or

31. Dehmer, J.L.; and Dill, D. Phys. Rev. Lett. (1975), 35, 213. See also ref. 29 for a complete discussion of this problem.
32. Herzberg, G. "Spectra of Diatomic Molecules" D. Van Nostrand Corp. Inc. Princeton, NJ 1950. This book contains an extensive discussion of spectra of diatomic molecules and the intensities in electronic-vibrational transitions.
33. West, J.B.; Parr, A.C.; Cole, B.E.; Ederer, D.L.; Stockbauer, R.L.; Dehmer, J.L. J. Phys. B (1980), 13, L105.
34. Dehmer, J.L.; Dill D.; Wallace, S. Phys. Rev. Lett. (1979) 43, 1005.
35. Lucchese, R.R. and McKoy, B.V. J. Phys. Chem. (1980), 85, 2166.
36. Gardner, J.L. and Samson, J.A.R. J. Electron. Spectrosc. (1978), 13, 7.
37. Carlson, T.C.; Krause, M.O.; Mehaffy, D.; Taylor, J.W.; Grimm, F.; Allen, J.D. J. Chem. Phys., (1980), 73, 6056.
38. Robert D. Cowan "The Theory of Atomic Structure and Spectra." The University of California Press, Berkeley 1981. The scientific literature on autoionization is extensive, dating back several decades. This reference offers an excellent summary with appropriate reference to the original literature.

39. Dehmer, P.M. and Chupka, W.A. Argonne National Laboratory Report ANL 77-65 (1977) p. 28
40. Hopfield, J.J. Phys. Rev., (1930). 35, 1133.
ibid, (1930), 36, 789.
41. Raoult, M.; LeRouzo, H.; Raseev, G.; and Lefebvre-Brion, H. J. Phys. B (1983), 16 4601.
42. Stern, E.A. and Heald, S.M. "Basic Principles and Applications of EXAFS" chapter 10 in Ref. 9.
43. Eastman, D.E.; Denelon, J.J.; Hien, N.C.; and Himpsel, F.J., Nucl. Inst. Meth. (1980), 172, 327.
44. See also review by Madey, T.E. and Stockbauer, R. "Methods of Experimental Physics: Vol 22", Academic Press, New York (1985).
45. Knotek, M.L., Rep. Prog. Phys. (1984) 47, 1499.
46. Menzel, D. and Gomer, R. J. Chem. Phys., (1964) 41, 3311,
Redhead, D.A., Can. J. Phys. (1964), 42, 886.
47. Knotek, M. and Feibelman, P.J. Phys. Rev. Lett. (1978) 40
964, Surf. Sci. (1979), 90, 78.
48. Madey, T.E.; Stockbauer, R.S.; Van der Veen, J. F.;
Eastman, D.E. Phys. Rev. Lett., (1980) 48, 187.
49. Stockbauer, R.; Hanson, D.; Flodstrom, S.A.; Madey, T.E.;
Phys. Rev. B. (1982, 26, 1885.
50. Winick, H.; Brown, G.; Halbach, K.; Harris, J. Physics Today, May 1981, Page 50. "Wiggler and Undulator Magnets".

Flow Injection Analysis: A New Concept of Microchemical Laboratory

Jaromir Ruzicka*

Chemistry Department A, The Technical University of Denmark, Lyngby, Denmark.

Although it is only a few years old, flow injection analysis (FIA) has established itself as a simple and automated method for the analysis of chemical solutions. So far, the method has been applied to a wide variety of chemical species. The purpose of the present paper is to review the present status of FIA.

Principles

The simplest FIA system consists of a peristaltic pump (P), a reagent reservoir (R) and a detector (D).

* Present address: Department of Chemistry, University of Washington, Seattle, WA 98195.